Front. Optoelectron. 2016, 9(3): 412–419
DOI 10.1007/s12200-016-0580-9

RESEARCH ARTICLE

Investigation of mode characteristics in rectangular microresonators for wide and continuous wavelength tuning

Mingying TANG, Shaoshuai SUI, Yuede YANG, Jinlong XIAO, Yun DU, Yongzhen HUANG (✉)

State Key Laboratory on Integrated Optoelectronics, Institute of Semiconductors, Chinese Academy of Sciences, Beijing 100083, China

Abstract The mode characteristics are investigated for the rectangular microresonators with an output waveguide connected to the midpoint of the long side for wide and continuous wavelength tuning. Through adjusting the aspect ratio of the rectangular microresonator, the mode Q factors can be greatly enhanced. Furthermore, the large mode interval between the high-Q modes makes the rectangular microresonators suitable for tunable lasers. As a special case, single-mode operation is achieved with a continuous tuning range of 9.1 nm for a square microlaser with the side length of 17.8 μm and the output waveguide width of 1.8 μm.

Keywords rectangular microresonator, semiconductor laser, tunable laser

1 Introduction

With the small size and high mode Q factor, microresonator lasers are potential light sources for photonic integrated circuits and optical interconnects [1–19]. In recent decades, varieties of microlasers have been investigated and demonstrated, such as circular microlasers [1–6], square microlasers [7–12] and other equilateral polygon microlasers [13–18]. Through connecting an output waveguide to the microresonators, single mode microlasers with unidirectional emission have been demonstrated [5,6,10–14]. Furthermore, single mode lasing without mode hopping was realized through adjusting the position and width of the output waveguide [12]. High-Q coupled modes can be obtained for the perfect rectangular microresonators with proper length and width [19].

In this paper, the mode characteristics are investigated for the rectangular microresonators using the two-dimensional (2D) finite-difference time-domain (FDTD) technique. An output waveguide is connected to the midpoint of the long side for unidirectional emission and mode selection. High-Q modes with large mode interval suitable for wide and continuous wavelength tuning can be obtained via proper design of the rectangle aspect ratio and the output waveguide width. This paper is organized as follows. In Section 2, we give the numerical model for the simulation of rectangular microresonators. In Section 3, we investigate the influences of the aspect ratio of the rectangular microresonator on the mode characteristics through fixing the area of the microresonator. In Section 4, the influences of the output waveguide width on the mode characteristics are investigated. In Section 5, the characteristics of square microlaser as a special case for the rectangular microlasers are reported, and finally the conclusion is summarized in Section 6.

Received December 29, 2015; accepted February 3, 2016

E-mail: yzhuang@semi.ac.cn

2 Numerical model

The mode characteristics for the rectangular microresonator, with an output waveguide connected to the midpoint of the long side, are numerically investigated by 2D FDTD technique. The 2D schematic diagram of the rectangular microresonator is presented in Fig. 1, where a and b are the width and length of the microresonator, respectively, and w is the width of the output waveguide. As shown in Fig. 1, the rectangular microresonator is laterally confined by benzocyclobutene (BCB), and a 200-nm silicon nitride (SiN_x) is sandwiched between them as the adhesion layer. The refractive indices of AlGaInAs/InP laser wafer, SiN_x and BCB layers are taken to be 3.2, 2 and 1.54, respectively. The spatial steps Δx and Δy are set to be 20 nm and the time step is fixed to be 0.0467 fs based on the Courant limit. A 50-cell perfectly matched layer (PML) absorbing boundary condition is applied to terminate the simulation area. A cosine impulse modulated by a

Gaussian function $P(t) = \exp[-(t-t_0)^2/t_w^2]\cos(2\pi f_0 t)$ is used as the exciting source, with the pulse center $t_0 = 6.6$ fs, the pulse half width $t_w = 19.8$ fs, and the pulse center frequency $f_0 = 193.5$ THz. Symmetric and antisymmetric excitation sources are used to simulate symmetric and antisymmetric modes relative to the middle line of the output waveguide, respectively. The variations of H_z are recorded as the FDTD outputs for the transverse-electric (TE) modes, and then the outputs are transformed from the time domain to frequency domain using Padé approximation [20]. Through fitting the resonance peak with a Lorentzian function, the mode wavelengths and Q factors can be obtained.

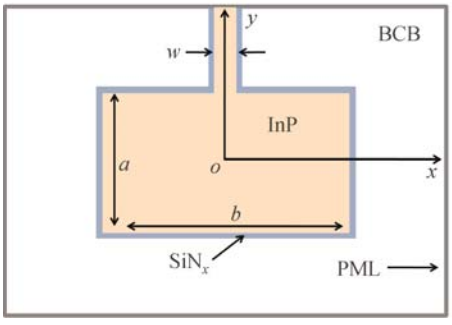

Fig. 1 2D schematic diagram of the rectangular microresonator with an output waveguide connected to the midpoint of the long side

3 Influences of rectangle aspect ratio on the mode characteristics

3.1 Rectangular microresonators with $S = 100$ μm^2

The mode characteristics are investigated for the rectangular microresonators with the area $S = 100$ μm^2 and the width of the output waveguide $w = 1$ μm. The mode Q factors for the symmetric and antisymmetric modes, with the highest mode Q factors of the modes with the wavelengths ranging from 1450 to 1650 nm, are presented in Fig. 2(a) for the rectangular microresonators with b/a ranging from 1 (square microresonator) to 2.4 at a step of 0.1. The mode Q factors for the symmetric and antisymmetric modes first change slightly when b/a is less than 1.6 and then increase rapidly as $1.6 < b/a < 1.8$. As $b/a = 1.8$, the mode Q factor for the symmetric mode is almost four times of that at $b/a = 1$ while the mode Q factor for the antisymmetric mode double that at $b/a = 1$. Moreover, the mode Q factor for the symmetric mode is much higher than the antisymmetric mode as $b/a = 1.8$. As b/a continues to increase, the mode Q factors decrease gradually except for the kink at $b/a = 2$ for the symmetric mode. Furthermore, the mode field distributions for the symmetric modes are calculated and plotted in Figs. 2(b)–2(e) at $b/a = 1$, 1.4, 1.8 and 2.1, respectively, where the field distributions in the output waveguide are magnified by 5 times.

Based on the mode field distributions and the simulation results in Ref. [19], the high-Q modes in the rectangular

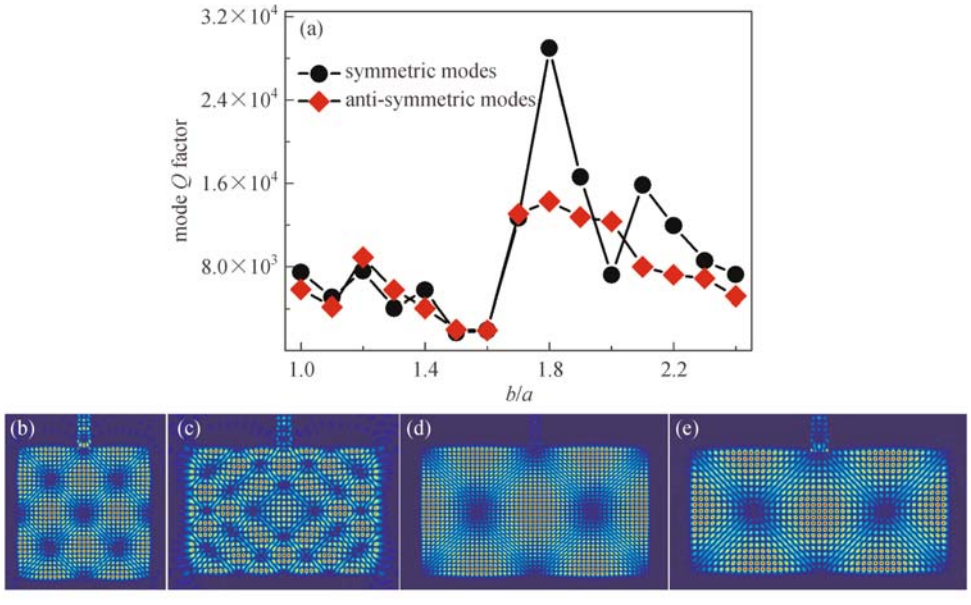

Fig. 2 (a) Mode Q factors for the symmetric and antisymmetric modes, with the highest mode Q factors of the modes with the wavelengths ranging from 1450 to 1650 nm for the rectangular microresonator with b/a ranging from 1 to 2.4 at a step of 0.1 as $S = 100$ μm^2 and $w = 1$ μm, and the mode field distributions for the corresponding symmetric modes in the rectangular microresonators at b/a of (b) 1, (c) 1.4, (d) 1.8 and (e) 2.1, respectively. The field distributions in the output waveguide are magnified by 5 times and the proportional scales of (b)–(e) are different

microresonators are coupled modes from two original modes $TE^{(p_1,q_1)}$ and $TE^{(p_2,q_2)}$ with the same symmetries and close wavelengths. The mode order number for the coupled modes in the rectangular microresonator can be assigned by the wave nodes number along the long side. Due to the strong mode field distribution in the midpoint of the long side, the fundamental modes are suppressed by the midpoint-connected output waveguide [11]. Therefore, the first-order transverse mode has the highest mode Q factor in the rectangular microresonators with an output waveguide connected to the midpoint of the long side if it can be obtained. For the first-order transverse coupled modes, the mode numbers of the original modes $TE^{(p_1,q_1)}$ and $TE^{(p_2,q_2)}$ have the relation of

$$|q_1 - q_2| = 4. \tag{1}$$

Based on the mode analysis in Ref. [12], the propagation constants in the x and y directions k_x and k_y for the modes $TE^{(p,q)}$ in the rectangular microresonators can be estimated from

$$k_x \approx (q+1)*pi/b, \tag{2}$$

$$k_y \approx (p+1)*pi/a. \tag{3}$$

For the high-Q coupled modes, the incident angles of the original modes are close to 45°, which indicates k_x is close to k_y. Therefore, the mode numbers of the original modes $TE^{(p_1,q_1)}$ and $TE^{(p_2,q_2)}$ with close wavelengths have the relation of

$$|p_1 - p_2|/a = |q_1 - q_2|/b. \tag{4}$$

Since the original modes have the same symmetries, $|q_1 - q_2|$ will be an even number. To obtain the high-Q first order transverse mode, a and b have to satisfy the following relation

$$b \approx l*a,\ l = 1,2. \tag{5}$$

The mode field distributions in Figs. 2(b), 2(d) and 2(e) show that the symmetric modes with the highest mode Q factors in the rectangular microresonators with b/a = 1, 1.8 and 2.1 are the first-order transverse modes, which are in well agreement with the above numerical analysis. At b/a = 1.4, Eq. (5) is not satisfied and thus the high Q mode is the higher-order mode, as shown in Fig. 2(c).

The mode intensity spectra for the symmetric and antisymmetric modes are presented in Figs. 3(a) and 3(b) for the square microresonator and the rectangular microresonator with b/a = 1.8, respectively. For the square microresonator with w = 1 μm, two high-Q symmetric modes are observed at the wavelengths of 1452.80 and 1553.53 nm. They are $TE^{o,(30,34)}$ and $TE^{o,(28,32)}$ modes with the mode Q factors of 9.93×10^3 and 7.51×10^3, respectively, corresponding to the first-order modes. The mode Q factors for the antisymmetric first-order modes $TE^{o,(29,33)}$ and $TE^{o,(27,31)}$ are 7.93×10^3 and 5.89×10^3, respectively, which are close to the adjacent symmetric first-order modes.

For the rectangular microresonator with w = 1 μm as b/a = 1.8, five high-Q symmetric modes are observed at the mode wavelengths of 1473.13, 1507.92, 1544.83, 1583.11 and 1623.64 nm, which are marked as C_1, C_2, C_3, C_4 and C_5. The corresponding mode Q factors for modes C_1, C_2, C_3, C_4 and C_5 are 2.90×10^4, 3.09×10^3, 9.17×10^3, 4.83×10^3 and 2.28×10^3, respectively, with the mode Q factor for mode C_1 much higher than the other four modes. For the antisymmetric modes, six high-Q modes are observed at the wavelengths of 1456.10, 1490.61, 1526.03, 1563.56, 1603.15 and 1644.56 nm. They are marked as D_1, D_2, D_3, D_4, D_5 and D_6, with the corresponding mode Q factors of 4.68×10^3, 4.03×10^3, 9.45×10^3, 2.75×10^3, 1.43×10^4 and 4.18×10^3, respectively. The mode Q factor for mode D_5 is larger than those of modes D_1, D_2, D_3, D_4 and D_6 but smaller than the symmetric mode C_1. Furthermore, the mode field distributions for modes C_1, C_3, D_3 and D_5 are calculated and plotted in Figs. 4(a)–4(d), respectively, which are magnified by 5 times in the output waveguide. Through applying Fourier transform on the mode field distributions, the mode numbers of the original modes can

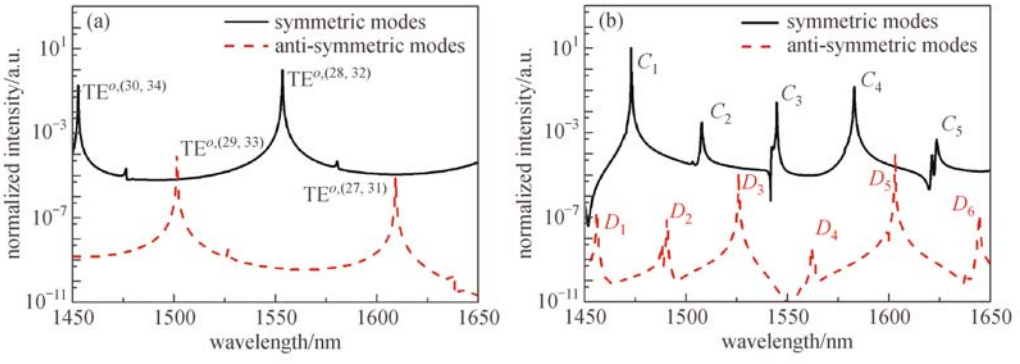

Fig. 3 Mode intensity spectra for the symmetric modes and antisymmetric modes in (a) the square microresonators and (b) the rectangular microresonators with b/a = 1.8 as S = 100 μm^2 and w = 1 μm

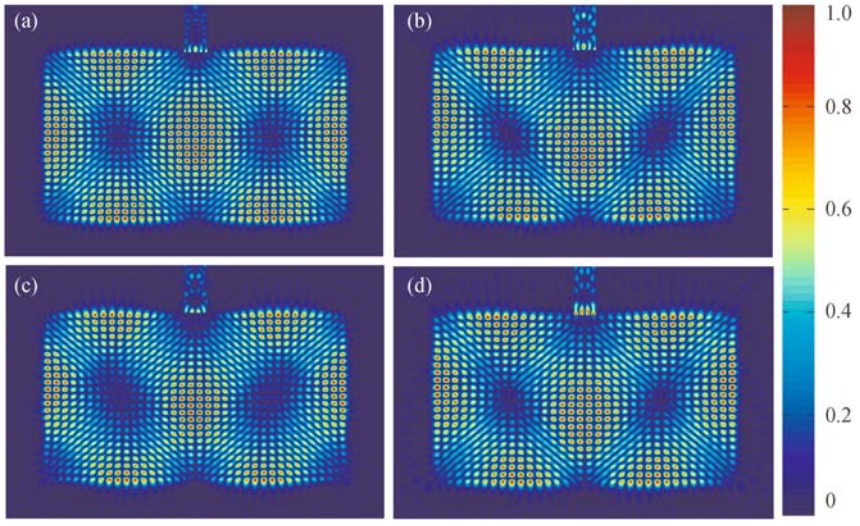

Fig. 4 Mode field distributions for the symmetric modes (a) C_1 and (b) C_3, and antisymmetric modes (c) D_3 and (d) D_5 in the rectangular microresonator with b/a = 1.8 and w = 1 μm. The field distributions in the output waveguide are magnified by 5 times

be obtained [11] and they are summarized in Table 1 for modes C_1, C_2, C_3, C_4, C_5, D_1, D_2, D_3, D_4, D_5 and D_6. The mode numbers (p_1,q_1) and (p_2,q_2) for the original modes $TE^{(p_1,q_1)}$ and $TE^{(p_2,q_2)}$ have the relation of $|q_1 - q_2| = 4$, which indicates that modes C_1, C_2, C_3, C_4, C_5, D_1, D_2, D_3, D_4, D_5 and D_6 are the first-order modes. Different from the square microresonator, the differences between the mode Q factors for the first-order modes in the rectangular microresonator is large, and this may be induced by different k_x/k_y of the original mode. For mode C_1, k_x/k_y of the original modes $TE^{(23,34)}$ and $TE^{(21,38)}$ are 1.21 and 1.00, which indicates that the incident angles of the modes are close to 45°. Therefore, the mode Q factor for mode C_1 is much higher than the other first-order transverse modes, which makes the rectangular microresonators suitable for tunable lasers.

3.2 Rectangular microresonators with S = 144 μm^2

For the rectangular microresonators with S = 144 μm^2 and w = 1 μm, the mode Q factors versus b/a are presented in Fig. 5(a) for the symmetric and antisymmetric modes, with the highest mode Q factors of the modes with the wavelengths ranging from 1450 to 1650 nm, as b/a increases from 1 to 2.4 at a step of 0.1. The mode Q factors for the symmetric and antisymmetric modes decrease as $b/a < 1.6$. For the symmetric modes, the mode Q factors increase rapidly as $1.6 < b/a < 2.1$ except for the sharp kinks at b/a = 1.9 and 2. When b/a = 2.1, the mode Q factor for the symmetric mode is 9.26×10^4, which is almost five times of that at b/a = 1, and it is much higher than symmetric mode with the second highest mode Q factor of 4.22×10^4 and the corresponding antisymmetric modes. The large differences between the mode Q factors for different modes make the rectangular with b/a = 2.1 and w = 1 μm suitable for the tunable lasers. Furthermore, the mode filed distributions are presented Figs. 5(b) – 5(e) for the symmetric modes with the highest mode Q factors in the rectangular microresonators with b/a = 1, 1.4, 1.8 and 2.1, respectively, which are magnified by 5 times in the output waveguide. The four symmetric modes at b/a = 1, 1.4, 1.8 and 2.1 are marked as modes H, I, J, K, respectively. The mode field distributions show that modes H, J and K are the first-order modes while mode I is the third-order transverse mode, which agrees well with the numerical analysis in Section 3.1.

Table 1 Mode Q factors and original modes for the high-Q coupled modes in the rectangular microresonator with b/a = 1.8 and w = 1 μm

modes	Q factor	original modes	modes	Q factor	original modes
C_1	2.90×10^4	$TE^{(23,34)}$, $TE^{(21,38)}$	D_1	4.68×10^3	$TE^{(26,31)}$, $TE^{(24,35)}$
C_2	3.09×10^3	$TE^{(22,34)}$, $TE^{(20,38)}$	D_2	4.03×10^3	$TE^{(25,31)}$, $TE^{(23,35)}$
C_3	9.17×10^3	$TE^{(22,32)}$, $TE^{(20,36)}$	D_3	9.45×10^3	$TE^{(22,33)}$, $TE^{(20,37)}$
C_4	4.83×10^3	$TE^{(23,28)}$, $TE^{(21,32)}$	D_4	2.75×10^3	$TE^{(23,29)}$, $TE^{(21,33)}$
C_5	2.28×10^3	$TE^{(23,26)}$, $TE^{(21,30)}$	D_5	1.43×10^4	$TE^{(22,29)}$, $TE^{(20,33)}$
			D_6	4.18×10^3	$TE^{(23,25)}$, $TE^{(21,29)}$

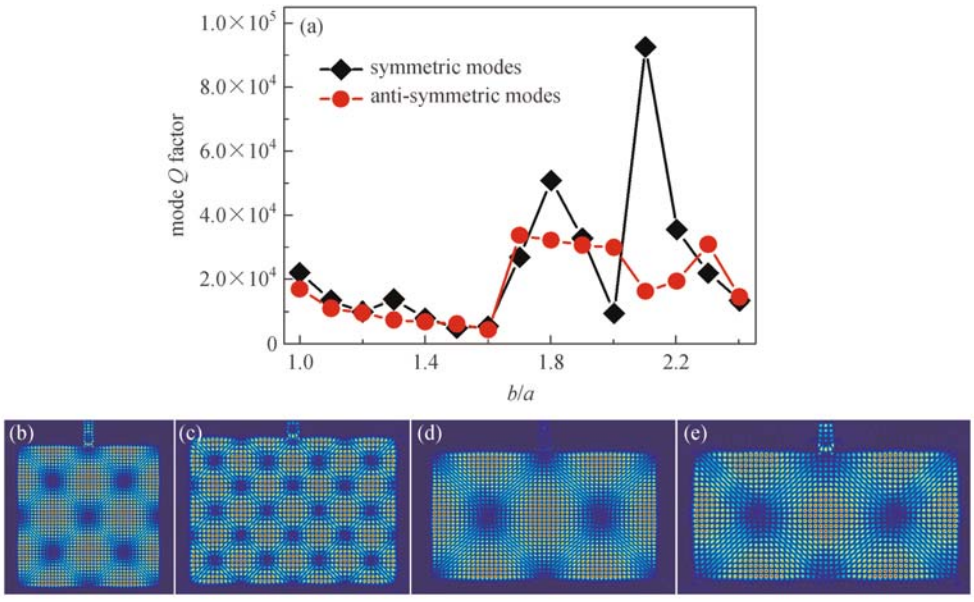

Fig. 5 Mode Q factors for the symmetric and antisymmetric modes (a), with the highest mode Q factors of the modes with the wavelengths ranging from 1450 to 1650 nm for the rectangular microresonator with b/a ranging from 1 to 2.4 at a step of 0.1 as $S = 144$ μm^2 and $w = 1$ μm. and the mode field distributions for the corresponding symmetric modes in the rectangular microresonators at b/a of (b) 1, (c) 1.4, (d) 1.8 and (e) 2.1, respectively. The field distributions in the output waveguide are magnified by 5 times and the proportional scales of (b)–(e) are different

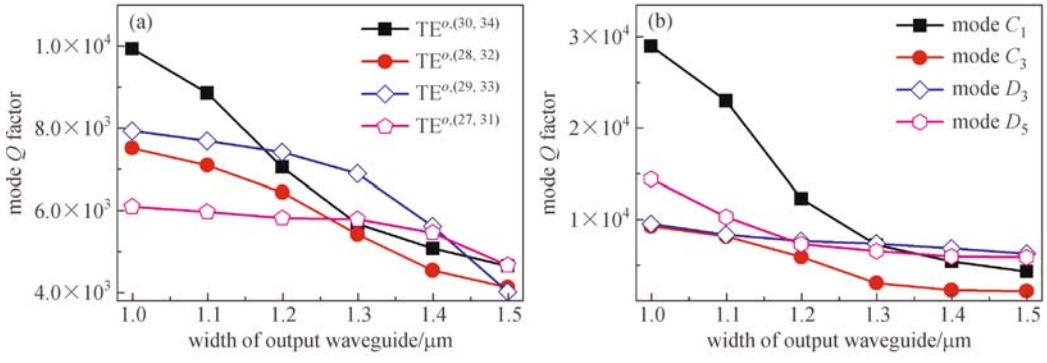

Fig. 6 Mode Q factors versus the output waveguide width for (a) modes TE$^{o,(30,34)}$, TE$^{o,(28,32)}$, TE$^{o,(29,33)}$ and TE$^{o,(27,31)}$ in the square microresonator and (b) modes C_1, C_3, D_3 and D_5 in the rectangular microresonators with $b/a = 1.8$ as $S = 100$ μm^2

4 Influences of the output waveguide width on the mode Q factors

The influences of the output waveguide are investigated for the square microresonator and the rectangular microresonator with $b/a = 1.8$ as $S = 100$ μm^2. The mode Q factors versus the output waveguide width w are presented in Fig. 6(a) for the symmetric modes TE$^{o,(30,34)}$ and TE$^{o,(28,32)}$ and antisymmetric modes TE$^{o,(29,33)}$ and TE$^{o,(27,31)}$ in the square microresonator. The mode Q factors for the symmetric and antisymmetric modes decrease with w and they are close to each other under different output waveguide widths. As shown in Fig. 6(b), the mode Q factor for the high-Q symmetric mode C_1 decreases rapidly from 2.90×10^4 to 7.13×10^3 due to the increase of the coupling loss caused by the output waveguide as w increases from 1 to 1.3 μm. When $w > 1.3$ μm, the mode Q factors for modes C_1, C_3, D_3 and D_5 are close to each other and the small mode interval between these modes makes the rectangular unsuitable for the tunable lasers.

5 Output characteristics of square microlasers

The output characteristics are tested for the square

microlasers laterally confined by BCB. For a square microlaser with the side length of 17.8 μm and the output waveguide width of 1.8 μm, the output power is measured by butt-coupling a multi-mode fiber to the cleaved facet of the output waveguide and presented in Fig. 7(a). The threshold current is about 4.5 mA at 291 K and the corresponding threshold current density is 1.42 kA/cm^2. From the *I*-*V* curve around the threshold current, a series resistor of 24.2 Ω is estimated.

The lasing spectra are measured and plotted in Fig. 7(b) at the injection currents of 5, 15, 25, 35, 45, 55 and 59 mA, respectively, where the adjacent lasing spectra are relatively shifted by 10 dB for clarity. As I = 5 mA, three evident peaks are observed at the wavelengths of 1518.39, 1531.22 and 1544.31 nm at 291 K with the wavelength intervals of 12.83 and 13.09 nm, respectively, which can be fitted by the longitudinal mode interval $\lambda^2/2^{3/2}/a/n_g$ with the group index n_g of 3.59. The dominant lasing mode is mode A with the side mode suppression ration (SMSR) of 18 dB at 5 mA, and it jumps 27.1 nm over two longitudinal mode intervals to mode C with an additional thermal-induced wavelength redshift of 1.1 nm as I increases to 15 mA. This indicates that mode C has a higher mode Q factor than mode B and the mode interval between the adjacent high-Q modes for the square microresonator is twice of the longitudinal mode interval, which agrees well with the simulation results in Fig. 3(a). As the injection current continues to increase, the dominant lasing mode keeps constant at mode C because of the high mode Q factor and large mode interval for the high-Q modes. Therefore, the lasing wavelength can be tuned continuously through tuning the injection current. The mode wavelengths and SMSR versus the continuous wave (CW) injection currents are summarized in Fig. 7(c) at 291 K. As shown in Figs. 7(b) and 7(c), the mode wavelength can be continuously tuned from 1545.4 to 1554.51 nm with the SMSR larger than 26 dB as I increases from 15 to 59 mA, and the corresponding wavelength tuning range is 9.11 nm. The influences of the injection current on the lasing wavelength can be mainly contributed to three mechanisms, which are carrier-induced variation of refractive index, thermal expansion of the device and the temperature-induced variation of refractive index. Since the carrier density of the microlaser almost keeps constant as the injection current is larger than the threshold current, the carrier-induced variation of refractive index is small and it has slight influence on the lasing wavelength. The lasing wavelength shift caused by the thermal expansion and the temperature-induced variation of refractive index on the lasing wavelength is almost linear to the temperature of the microlaser [21]. Under a pulsed current with a pulse duty of 1% and a pulse width of 10 ns, the mode wavelength redshift rate of 0.114 nm/K is obtained by varying the thermoelectric cooler (TEC) temperature. When the injection current and the TEC temperature are fixed at certain values, the temperature of the microlaser almost keeps constant, and thus the refractive index seldom changes. Therefore, the lasing wavelength almost keeps constant at certain injection current and the wavelength tuning can be repeated.

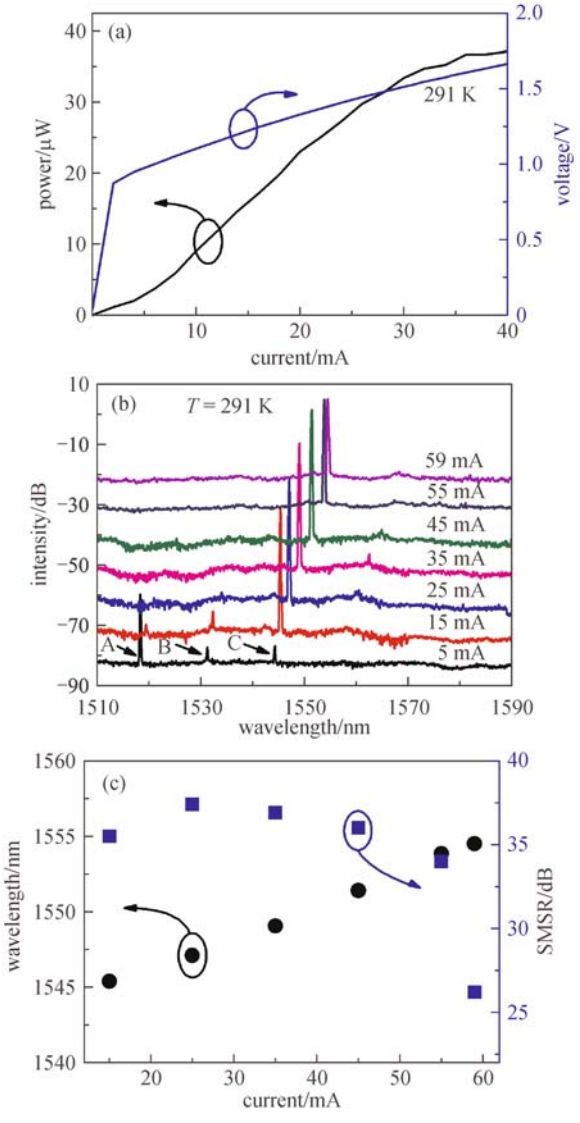

Fig. 7 (a) Output power and applied voltage versus CW injection current at 291 K, (b) lasing spectra at different currents at 291 K, and (c) lasing wavelength and SMSR versus the current at 291 K, for the square microlaser with the side length of 17.8 μm and the output waveguide width of 1.8 μm

6 Conclusions

In conclusion, the mode characteristics are investigated for the rectangular microresonators with an output waveguide connected to the midpoint of the long side. For a rectangular microresonator with fixed area, the mode Q factors can be greatly enhanced through choosing the rectangular aspect ratio. As the aspect ratio is around 2,

mode Q factors are much higher than the corresponding square microresonator for the rectangular microresonator with a 1-μm-width output waveguide. Furthermore, the influences of the output waveguide width are investigated. When the width of the output waveguide is less than 1.2 μm, the rectangular microresonators are suitable for tunable lasers due to the large difference between the adjacent modes with the same transverse mode number and the large mode interval. The square microresonators with the mode interval for the high-Q modes twice of the longitudinal mode interval can also be utilized for the tunable lasers. For a square microlaser with the side length of 17.8 μm and the output waveguide width of 1.8 μm, single-mode operation is achieved with a continuous tuning range of 9.1 nm. With the compact size, the microlaser can provide compact tunable light source for the photonic integrated circuits and optical interconnects.

References

1. McCall S L, Levi A F J, Slusher R E, Pearton S J, Logan R A. Whispering-gallery mode microdisk lasers. Applied Physics Letters, 1992, 60(3): 289–291
2. Baba T, Yogo Y, Suzuki K, Koyama F, Iga K. Near room temperature continuous wave lasing characteristics of GaInAsP/InP surface emitting laser. Electronics Letters, 1993, 29(10): 913–914
3. Levi A F J, Slusher R E, Mccall S L, Glass J L, Pearton S J, Logan R A. Directional light coupling from microdisk lasers. Applied Physics Letters, 1993, 62(6): 561–563
4. Zhang Z, Yang L, Liu V, Hong T, Vahala K, Scherer A. Visible submicron microdisk lasers. Applied Physics Letters, 2007, 90(11): 111119–111121
5. Yang Y D, Wang S J, Huang Y Z. Investigation of mode coupling in a microdisk resonator for realizing directional emission. Optics Express, 2009, 17(25): 23010–23015
6. Wang S J, Lin J D, Huang Y Z, Yang Y D, Che K J, Xiao J L, Du Y, Fan Z C. AlGaInAs-InP microcylinder lasers connected with an output waveguide. IEEE Photonics Technology Letters, 2010, 22 (18): 1349–1351
7. Poon A W, Courvoisier F, Chang R K. Multimode resonances in square-shaped optical microcavities. Optics Letters, 2001, 26(9): 632–634
8. Boriskina S V, Benson T M, Sewell P, Nosich A I. Spectral shift and Q-change of circular and square-shaped optical microcavity modes due to periodic sidewall surface roughness. Journal of the Optical Society of America B: Optical Physics, 2005, 21(10): 1792–1796
9. Guo W H, Huang Y Z, Lu Q Y, Yu L J. Whispering-gallery-like modes in square resonators. IEEE Journal of Quantum Electronics, 2003, 39(9): 1106–1110
10. Che K J, Huang Y Z. Mode characteristics of metallically coated square microcavity connected with an output waveguide. Journal of Applied Physics, 2010, 107(11): 113103
11. Long H, Huang Y Z, Yang Y D, Zou L X, Lv X M, Liu B W, Xiao J L, Du Y. Mode characteristics of unidirectional emission AlGaInAs/InP square resonator microlasers. IEEE Journal of Quantum Electronics, 2014, 50(12): 981–989
12. Tang M Y, Sui S S, Yang Y D, Xiao J L, Du Y, Huang Y Z. Mode selection in square resonator microlasers for widely tunable single mode lasing. Optics Express, 2015, 23(21): 27739–27750
13. Lin J D, Huang Y Z, Yang Y D, Yao Q F, Lv X M, Xiao J L, Du Y. Single transverse whispering-gallery mode AlGaInAs/InP hexagonal resonator microlasers. IEEE Photonics Journal, 2011, 3(4): 756–764
14. Zou L X, Lv X M, Huang Y Z, Long H, Xiao J L, Yao Q F, Lin J D, Du Y. Mode analysis for unidirectional emission AlGaInAs/InP octagonal resonator microlasers. IEEE Journal of Selected Topics in Quantum Electronics, 2013, 19(4): 1501808
15. Huang Y Z, Chen Q, Guo W H, Lu Q Y, Yu L J. Mode characteristics for equilateral triangle optical resonators. IEEE Journal of Selected Topics in Quantum Electronics, 2006, 12(1): 59–65
16. Huang Y Z, Hu Y H, Chen Q, Wang S J, Du Y, Fan Z C. Room-temperature continuous-wave electrically injected InP-GaInAsP equilateral-triangle-resonator lasers. IEEE Photonics Technology Letters, 2007, 19(13): 963–965
17. Ni C Y A, Chang S W, Gargas D J, Moore M C, Yang P D, Chuang S L. Metal-coated zinc oxide nanocavities. IEEE Journal of Quantum Electronics, 2011, 47(2): 245–251
18. Zhang C, Zhang F, Sun X W, Yang Y, Wang J, Xu J. Frequency-upconverted whispering-gallery-mode lasing in ZnO hexagonal nanodisks. Optics Letters, 2009, 34(21): 3349–3351
19. Yang Y D, Huang Y Z. Mode analysis and Q-factor enhancement due to mode coupling in rectangular resonators. IEEE Journal of Quantum Electronics, 2007, 43(6): 497–502
20. Guo W H, Li W J, Huang Y Z. Computation of resonant frequencies and quality factors of cavities by FDTD technique and Pade approximation. IEEE Microwave and Wireless Components Letters, 2001, 11(5): 223–225
21. Mccaulley J A, Donnelly V M, Vernon M, Taha I.Temperature dependence of the near-infrared refractive index of silicon, gallium arsenide, and indium phosphide. Physical Review B: Condensed Matter, 1994, 49(11): 7408–7417

Mingying Tang received the B.S. degree from Huazhong University of Science and Technology, Wuhan, China, in 2011. She is currently pursuing the Ph.D. degree at Institute of Semiconductors, Chinese Academy of Sciences, Beijing, China. She is working on the design and fabrication of microlasers.

Shaoshuai Sui received the B.S. degree in physics from Qingdao University, Qingdao, China, in 2011. He is currently pursuing the Ph.D. degree with the Institute of Semiconductors, Chinese Academy of Sciences, Beijing, China, and is involved in silicon photonics.

Yuede Yang received the B.S. degree in physics from Peking University, Beijing, China, in 2004, and the Ph.D. degree in physical electronics from the Institute of Semiconductors, Chinese Academy of Sciences, Beijing, in 2009. Since 2009, he has been an Assistant Professor with the Institute of Semiconductors, Chinese Academy of Sciences. His current research interest is in the design and the fabrication of microcavity lasers and filters.

Jinlong Xiao received the B.S. and M.S. degrees from Chongqing University, Chongqing, China, in 1999 and 2002, respectively, and the Ph.D. degree from the Institute of Semiconductors, Chinese Academy of Sciences, Beijing, China, in 2008. His research interests are in the simulation and fabrication of quantum dot microcavity lasers and semiconductor optical amplifiers.

Yun Du received the Graduate degree from the College of Continued Education, Chinese Academy of Sciences (CAS), Beijing, in 1990. In 1984, she joined the Institute of Semiconductors, CAS, where she was engaged in research on the technique process of semiconductor optoelectronic devices, and has been a Senior Process Technician since 2007.

Yongzhen Huang received the B.Sc., M.Sc., and Ph.D. degrees in physics from Peking University, Beijing, China, in 1983, 1986, and 1989, respectively. In 1989, he joined the Institute of Semiconductors, Chinese Academy of Sciences, Beijing, China, where he worked on the tunneling time for quantum barriers, asymmetric Fabry–Perot cavity light modulators, and VCSELs. In 1994, he was a visitor at BT Laboratories, Ipswich, UK, where he was involved in the fabrication of the 1550-nm InGaAsP VCSEL. Since 1997, he has been a Professor at the Institute of Semiconductors, Chinese Academy of Sciences, where he is also the Director of the Optoelectronic R&D Center. His current research interests are mainly focused on semiconductor microcavity lasers and photonic integrated circuits for optical interconnection.